

Control of cell division in the adult brain by heparan sulfates in fractones and vascular basement membranes

Vanessa Douet, Frederic Mercier

Department of Tropical Medicine, Medical Microbiology and Pharmacology, John A. Burns School of Medicine, University of Hawaii, Honolulu. HI96822

Short title: Fractones regulate cell division in the brain

Keywords for indexing: heparan sulfates, extracellular matrix, cell division, neural stem cell niche, fibroblast growth factor, bone morphogenetic protein

Abstract

Regulation of cell division in adult tissues and organs requires the coordination of growth factors at the surface of potentially-dividing cells in specific anatomic loci named germinal niches. However, the biological components and physiological system that control growth factors in the germinal niches are unknown. In the adult brain, no function has been attributed to fractones, the fractal-shaped extracellular matrix structures located in the subventricular zone (SVZ) next to neural stem and progenitor cells. Here, we show that BMP-7 (bone morphogenetic protein-7) and FGF-2 (fibroblast growth factor-2) modulate cell division in the SVZ only if the growth factors bind to heparan sulfates localized in fractones and adjoined vascular basement membranes. Our results strongly suggest that fractones and specialized basement membranes function as stem cell niche structures, capturing and potentiating growth factors to regulate cell division in the adult brain.

Introduction

We previously identified extracellular matrix (ECM) structures in the adult mammalian brain^{1,2} that differ from the three recognized categories of ECM, namely the interstitial matrix, the basement membrane and the glycocalyx³⁻⁶. This new ECM consists of myriads of individual fractal-shaped microstructures that we have named fractones¹. The fractal structure⁷, unique amongst the ECM, allows each individual fractone to contact the processes of numerous

neighboring cells in a minimal space^{1,2}. This is illustrated here in Figs. 1a-1c. Due to their high electron density, the fractone ultrastructure is directly visible by transmission electron microscopy (Figs. 1b and 1c). However, fractones are too small to be visualized as fractals by light microscopy and appear as punctae after fluorescence immunolabeling for laminin (Fig. 1f), nidogen, collagen-IV or heparan sulfate proteoglycans (HSPG) (Fig. 1d) and^{1,2,8}. These molecules are also found in basement membranes⁹⁻¹¹, the specialized mats of ECM that interface connective tissue with the parenchyma of organs and tissues. Thus, despite their unique morphology, fractones chemically resemble basement membranes.

In the adult mammalian brain, fractones are exclusively located in the walls bordering the ventricles, assembled in series at the interface between the ependyma and the subventricular zone (SVZ) (Figs. 1d-1f). The distribution of fractones and their arrangement through the SVZ is best visualized tangentially to the ventricular surface after immunolabeling for its ECM molecules (Fig. 1f). Fractones are similarly distributed throughout the brain ventricular system and spinal subependyma^{1,2,8}.

We are just beginning to investigate the function of fractones. We have previously shown that fractones directly contact neuroblasts and potential neural stem cells in the SVZ of the anterior lateral ventricle (SVZa)¹, the principal residence of neural stem cells^{12,13} and a major neurogenic zone in adulthood^{14,17}. The SVZa is responsible for the generation of both neurons and glia, which then migrate to colonize other brain zones¹⁸. We also demonstrated that fractones and specialized blood vessels of the SVZa specifically capture and concentrate the mitotic/neurogenic factor fibroblast growth factor-2 (FGF-2) *in vivo*⁸. Based on these findings, we hypothesize that fractones participate to the regulation of cell division and cell differentiation in the SVZa. It is anticipated that regulation of cell division and cell differentiation by growth factors requires mechanisms of selection, activation and coordination of growth factors in the stem cell niches. Fractones and other ECM may perform this function via HSPG and chondroitin sulfate proteoglycans (CSPG). It is known that HSPG located in the extracellular space capture, store and target growth factors such as fibroblast growth factor-2 (FGF-2), granulocyte macrophage colony stimulating factor (GM-CSF) and bone morphogenetic protein-4 (BMP-4) towards cell surface receptors to control mitosis and cell differentiation¹⁹⁻²⁴. Nearly all growth factors, cytokines and chemokines are heparin-binding molecules, therefore potentially depend upon extracellular HSPG to recognize their cognate receptors at the cell surface. Do fractones

and basement membranes coordinate growth factor signaling through their HSPG to modulate cell proliferation and cell differentiation in the stem cell niches?

Here, we focused our work on the role of heparan sulfates, concentrated in fractones and vascular basement membranes, as potential regulators of cell division in the adult neural stem cell niche. We used intracerebral injections of growth factors, heparan sulfate deglycanation *in vivo* by heparitinase-1, mapping growth factor binding *in situ*, immunolabeling for heparan sulfates and quantification of cell division by bromodeoxyuridine (BrdU) immunolabelings to investigate the role of fractones and vascular basement membranes in the SVZa. Herein, we demonstrate that BMP-7 and FGF-2 must bind heparan sulfates present in fractones and vascular basement membranes to respectively inhibit and stimulate cell division in the SVZa.

Results

Fractones and vascular basement membranes of the SVZa capture BMP-7

To investigate the potential of fractones to capture growth factors, we intracerebroventricularly (ICV) injected BMP-7 tagged with biotin in the adult mouse brain. The sites of capture (binding) of biotinylated-BMP-7 were visualized with streptavidin Texas red on frozen sections of the brain, 22 hours after injection. Figure 2a shows biotinylated BMP-7 concentrated as punctae in the SVZa, a diffuse pattern in the choroid plexus, and no detectable binding elsewhere. Immunolabeling for the ECM marker N-sulfates heparan sulfates (NS-HS, antibody 10E4) (Fig. 2b), a specific specific for fractones, meninges and rare blood vessels (primarily those of the SVZa)⁸, indicated a correspondence between BMP-7 binding sites and 10E4 immunoreactivity (compare Figs. 2a and 2b). Magnified fields in Figs. 2c and 2d revealed that the majority of BMP-7 binding sites were sharp punctae with a diameter $< 5 \mu\text{m}$ corresponding to fractones. However, we also detected BMP-7 binding sites/10E4 immunolabeled structures that correspond to the typical cylindrical pattern of blood vessels with a diameter $> 6 \mu\text{m}$. The distinction between fractones and blood vessels of the SVZa by the morphological pattern of 10E4 or laminin immunolabeling is discussed in our previous publications^{1,2,8}. The strict coincidence between the binding sites of BMP-7 and immunolabeling for 10E4 strongly suggests that BMP-7 binds to fractones and to the basement membranes of blood vessels supplying the SVZa. The position of vascular basement membranes within the

blood vessel walls and the typical branched pattern of vascular basement membranes in the SVZa are documented in our previous publications^{1, 25, 26}.

Interestingly, blood vessels located beyond the SVZa did not significantly bind BMP-7, as illustrated by the absence of detectable binding in the corpus callosum or fimbria hippocampus in Fig. 2a. Therefore, BMP-7 specifically bound to blood vessels in the SVZa, immunoreactive for NS-HS and visualized with the antibody 10E4. Figures 2h and 2i show that BMP-7 was also concentrated by fractones and vascular basement membranes in the walls of the fourth ventricle (arrow) and meninges projecting to the fourth ventricle (arrowhead). BMP-7 binding occurred in fractones of the third ventricle as well (not shown).

Co-localisation of BMP-7 binding sites with N-sulfated heparan sulfate domains

Deglycanation by heparitinase-1 was used to cleave heparan sulfate chains *in vivo* and to determine whether the binding of BMP-7 to fractones and SVZa blood vessels still occurs without heparan sulfates. Under these experimental conditions, the binding of BMP-7 disappeared completely from fractones and blood vessels (Fig. 2f). This strongly suggests that the binding of BMP-7 occurred via heparan sulfates.

BMP-7 inhibits cell division *in vivo* in the SVZa

We next determined the effect of BMP-7 on cell proliferation in the SVZa. BMP-7 is an inhibitor of NSC proliferation *in vitro*²⁷, but to our knowledge, BMP-7's anti-neurogenic activity has not been demonstrated *in vivo*. Two single injections of BMP-7 were performed in adult mice, and the effect on cell proliferation measured four days after the first injection. To visualize cells that initiate mitosis (DNA replication, phase S), a single intraperitoneal injection of bromodeoxyuridine (BrdU) was performed six hours prior to animal termination. BrdU-immunoreactive cells were counted on series of coronal frozen sections containing the anterior portion of the lateral ventricle, each series on a minimum of three animals. Figures 3a and 3b show that BMP-7 strongly inhibited mitosis phase S in the SVZa. A reduction of cell proliferation by a factor of 3.5 was observed relative to the control (ICV injection with artificial CSF, Fig. 3a). Average values for cell counts throughout brain sections are reported in Fig. 3d and Table 1 (supplementary results). We did not observe significant cell count differences in the

ipsi- and contra-lateral ventricles. This indicated that BMP-7 penetrated the brain and equally inhibited cell division on both sides.

BMP-7 cannot efficiently inhibit cell proliferation in the SVZa when co-injected with heparitinase-1

To determine whether BMP-7 binding to fractones and vascular basement membranes is required for BMP-7-induced inhibition of cell division in the SVZa, we prevented the binding of BMP-7 by deglycanation (performing two successive injections of both heparitinase-1 and BMP-7) prior to assessing cell proliferation in the SVZa. The loss of BMP-7 binding to fractones and SVZa blood vessels almost restored the basic rate of cell proliferation (Figs. 3c and 3d, and detailed cell counts in supplemental Table 1). This suggests that the inhibitory effect of BMP-7 on cell proliferation requires BMP-7 capture by fractones and vascular basement membranes. Although the binding of BMP-7 was more frequently visualized in fractones than in vascular basement membranes (Fig. 2), it is impossible to speculate on the relative role of fractones versus SVZa as crucial promoters of BMP-7 to mediate the inhibition on cell division in the SVZa. To determine the effect of heparitinase-1 on the physiological rate of cell proliferation in the SVZa, other groups of mice were treated with injection of heparitinase-1 only. Heparitinase-1 on its own induced a slight but significant increase of the basic rate of cell proliferation (Figs. 3A and 3D, and complete cell counts provided in Table 1). Since these experiments have been performed *in vivo*, it is likely that endogenous growth factors are affected by heparitinase-1, and therefore that our results reflect the cumulative effect of heparitinase-1 on the injected plus endogenous growth factors. An overall interpretation of the results is provided in the discussion of this manuscript.

Co-localisation of FGF-2 binding sites with N-sulfated heparan sulfate domains

We previously reported that FGF-2, a mitotic factor in the adult neural stem cell niche²⁸, exclusively binds to fractones and vascular basement membranes in the walls of the lateral ventricle in the adult mouse⁸. However, the location of FGF-2 binding along the ventricular system was not detailed and the possible co-localization of FGF-2 binding with immunoreactivity for N-sulfated heparan sulfate domains (antibody 10E4) was not investigated.

FGF-2 was biotinylated and ICV injected in groups of adult mice. The FGF-2 binding sites were detected in frozen sections of the brain with streptavidin Texas red. Figs. 4a and 4c show that FGF-2 has been exclusively captured by the majority of fractones, vascular basement membranes in the SVZa and the choroid plexus in the lateral ventricle. Figures 5a-5C demonstrate that FGF-2 has been captured by fractones and SVZa blood vessels along other ventricles as well. To determine whether the binding sites of FGF-2 coincide with those of N-sulfated heparan sulfates, brain sections originating from animals that were injected with biotinylated FGF-2 were immunolabeled with the antibody 10E4. FGF-2 binding and 10E4 immunolabeling coincided in the SVZa and choroid plexus (Figs. 4a and 4b) as indicated by the yellow color, overlap of 10E4 labeling (green) and FGF-2 binding (red) (Fig. 4c). In the SVZa, most FGF-2/10E4 immunolabeling was found in fractones, although vascular basement membranes were also visualized (Fig. 4c, arrowhead).

FGF-2 binding sites matched those of immunoreactivity for N-sulfated heparan sulfates, suggesting that FGF-2 binding occurs via NS-HS. To determine whether FGF-2 capture by fractones and basement membranes is heparan sulfate-dependant, we injected heparitinase-1 in the brain just prior to injecting biotinylated FGF-2. In these experimental conditions, biotinylated FGF-2 was not detected in the SVZa (Fig. 6a), whereas some faint labeling was still observed in the choroid plexus. This result indicates that FGF-2 is captured by fractones and adjoining basement membranes via heparan sulfates. The perfect match between NS-HS immunoreactivity and FGF-2 binding further suggests that N-sulfation might be of particular importance for the binding. However, since heparitinase-1 cuts the whole heparan sulfate domain of HSPG, it is impossible to determine whether this is the loss of N-sulfation or the loss of another sulfation pattern that precludes the binding of FGF-2.

FGF-2 binding to fractones and vascular basement membranes of the SVZa is independent from the site of intracerebral injection

To further explore the capacity of fractones and adjacent vascular basement membranes to specifically capture FGF-2, we injected biotinylated FGF-2 in the dorsal cortex, instead of ICV. In these conditions, FGF-2 was captured by NS-HS immunoreactive fractones in the SVZa of the lateral ventricle (Figs. 5d-5f). This further supports the view that the binding of FGF-2 to fractones is specific and independent from the site of injection in the brain. To investigate the

toxicity of deglycanation in vivo, we examined the dynamic of recovery of NS-HS domains after in vivo enzymatic degradation by heparitinase-1, using immunolabeling for 10E4. Figure 6d shows that immunoreactivity for 10E4 has fully recovered 48 hours after ICV injection of heparitinase-1. Therefore, our in vivo experimental protocol of deglycanation appears appropriate for examining the effect of the binding loss on cell division in the SVZa.

FGF-2 cannot efficiently stimulate cell proliferation in the SVZa when co-injected with heparitinase-1

Finally, to determine whether the mitotic effect of FGF-2 requires the binding of FGF-2 to fractones and SVZa basement membranes, we examined the effects of FGF-2 on cell division in the SVZa after injection of FGF-2 or after successive injections of heparitinase-1 and FGF-2. Cell division was analyzed by counting BrdU immunoreactive cells in the walls of the lateral ventricle, using serial coronal sections of the brain, which comprise the SVZa. FGF-2 injected alone generated a 390% increase in the rate of cell proliferation in the SVZa, compared to the basic rate (Figs. 7a and 7c). However, when FGF-2 binding was prevented by heparitinase-1 treatment, the rate of cell proliferation in the SVZa increased by only 50% (Fig. 7f). Complete BrdU-immunoreactive cell counts throughout the SVZa are reported in supplemental results, table 1 (serial sections cut in the coronal plane). We also performed additional experiments, using the same injections but on series of animals in which dividing cells were counted in sagittally-cut brain sections (supplemental results, table 2). The results were similar to those obtained for coronal sections. These results strongly support the view that FGF-2 binding to fractones and SVZa basement membranes is required for the mitogenic effect of FGF-2 in the SVZa. Fig. 8 illustrates the interpretation of these results as well as those found for BMP-7.

Discussion

The data from this study suggest that BMP-7 and FGF-2 must be captured by heparan sulfates located in fractones and SVZ basement membranes to modulate cell division in the SVZ neurogenic zone. We show in vivo that heparitinase-1 deglycanation eliminates the specific binding of both growth factors to fractones and SVZa basement membranes (Figs. 2 and 6). The loss of binding is correlated with reduced stimulatory effect of FGF-2 and reduced inhibitory effect of BMP-7 on cell proliferation in the SVZa (Figs. 3 and 7). Heparitinase-1 by itself

slightly increases the rate of cell division in the SVZa (Fig. 7 and supplemental tables). It is likely that heparitinase-1 prevents the activity of endogenous heparin-binding growth factors, which together with the injected growth factor contribute to the regulation of cell division in the SVZa. Therefore, the results may reflect the cumulative effect of the lack of binding of both exogenous and endogenous growth factors to heparan sulfates in fractones and SVZa basement membranes. Nevertheless, the high degree of stimulation (390% with FGF-2) and inhibition (370% with BMP-7) of cell division, together with the absence of detectable binding and the loss of effect of these growth factors on cell division after heparitinase-1 treatment strongly suggest that the binding of FGF-2 and BMP-7 to fractones and adjacent basement membranes is required for regulating cell division in the SVZa.

A remarkable finding is that most fractones of the SVZa collect BMP-7 and FGF-2 (Figs. 2 and 4). This indicates that an individual fractone can collect growth factors with opposite effects. This also suggests that fractones may play a major role as regulators of growth factors, balancing both an effect and its opposite to ultimately control the rate of cell division in the SVZ. We conclude that heparan sulfates contained at fractones and vascular basement membranes likely represent the critical effectors that potentiate BMP-7 and FGF-2 and therefore intervene in the bi-directional regulation of cell division in the primary germinal zone of the adult brain.

In this study, we have shown that FGF-2 and BMP-7 were partly captured by the stroma of the choroid plexus (Figs. 2a and 4a). A brain barrier, formed by a complete wall of tight junctions, exists between the stroma (made of meninges) and the epithelium of the choroid plexus²⁹. For this reason, BMP-7 and FGF-2 bound in the choroid plexus stroma cannot cross the barrier and influence the SVZ. However, the epithelium of the choroid plexus produces growth factors, including FGF-2^{30,31}. It is possible that the choroid plexus stroma influences cell division in the SVZa, indirectly via a growth factor cascade relayed by the epithelium.

The importance of heparan sulfates as ECM receptors potentiating growth factors at the site of capture has been previously emphasized. Heparan sulfates are linear polysaccharides with repeated disaccharide units containing N- and O- sulfate esters at various positions. In vivo, heparan sulfates occur as HSPG, with the heparan sulfates attached to a core protein such as glypicans³² and syndecans, anchored at the cell surface in the interstitial ECM, or perlecan, agrin and collagen XVIII in the basement membranes, the specialized mats of ECM present at the

interface of the connective tissue with the parenchyma of organs. We have previously identified the HSPG perlecan in fractones⁸.

Heparin-binding sites are found in a large number of proteins that operate as mediators and that intervene in the regulation of diverse functions such as cell division and differentiation, morphogenesis, inflammation and wound healing. These proteins include enzymes, protease and esterase inhibitors, pathogens (viral proteins), growth factors, cytokines, chemokines and morphogens. To bind their receptors at the cell surface, most mediators requires the presence of heparin- (or possibly chondroitin- or keratan-) sulfates present in glycosaminoglycans of the ECM, which serve as obligatory co-receptors. More than two decades ago, it became apparent that without binding to heparan sulfates, granulocyte macrophage colony stimulating factor (GM-CSF) cannot influence hematopoeisis^{19,20}. Soon after, it was demonstrated that FGF-2 must bind heparan sulfates, and in particular perlecan, to exert its effect^{21,22,33}. The tripartite molecular interactions involve the presentation of FGF-2 to FGFR (FGF receptor) by heparan sulfates, the activation of protein kinase cascades by FGFR and ultimately modulation of cell division. Additionally, the FGF/heparan sulfate complex enters the cell nucleus by endocytosis to directly influence genes that are responsible for cell division²³.

The interaction of heparan sulfates with mediators in the ECM is not restricted to activation of the cell-surface receptors. Heparan sulfates also protect mediators from enzymatic degradation and serve as storage for mediator delayed activation³⁴. A third role of heparan sulfates is to recruit and activate mediators at specific anatomical sites. Whereas several HSPG such as glypicans and syndecans are located in the interstitial matrix at the cell surface³², other HSPG, such as perlecan²², agrin³⁵ and collagen XVIII³⁶, are located in basement membranes at the interface of the connective tissue with parenchymal cells of any tissue or organ. In the brain, basement membranes are located at the interface of the meninges (brain connective tissue) with the glia limitans, and in the walls of blood vessels, where the adventitia represents the connective tissue^{1,2,26}. Which mediators rely upon heparan sulfates to recognize their cognate receptors on the cell surface? A high number of mediators, cytokines, chemokines and ECM molecules are heparin binding. Interstitial- as well as the basement membrane- HSPG, have been implicated as crucial co-receptors for interaction with a large variety of ligands including growth factors (FGF-1, FGF-2 and FGF-4^{21,22,33,37,38}), all other members of the FGF and BMP families, other growth factors such as VEGF (vascular endothelial growth factor), HB-EGF (heparin-binding epidermal

growth factor), neuregulin, chemokines (CC chemokines and CXC chemokines), cytokines IL (interleukins) and IFN (interferons) (H. Ibelgauft, *Cytokines and cells online pathfinder encyclopedia, heparin binding domain*), amphiregulin³⁹, GM-CSF^{19,20}, morphogens such as Shh (sonic hedgehog)⁴⁰, Noggin and Wnt as well as ephrins and ECM molecules such as fibronectin. Therefore, all these heparan sulfate binding molecules are candidates for binding/activating by basement membranes or other ECM structures such as fractones. This is an attractive possibility when knowing that these molecules regulate neurogenesis^{41,42}. For example, Shh affects cell proliferation in the postnatal and adult SVZ⁴³.

Interestingly, most vascular basement membranes (besides those of the SVZ) were neither immunoreactive for 10E4 nor capturing FGF-2 and BMP-7. This suggests that a subset of ECM, immunoreactive for NS-HS, comprising fractones, SVZ vascular basement membranes and choroid plexus, is responsible for FGF-2 and BMP-7 capture. It has been shown that defective N sulfation limits the binding of heparin-binding growth factors and well as their activity⁴⁴. Therefore, the location of NS-HS immunolabeling (Figs. 2, 4 and 5) may reflect potential niches for multiple growth factor binding.

The question arises as to how heparan sulfates discriminate growth factors throughout the SVZ. It is known that epimerases, sulfatases and sulfotransferases operate in the Golgi apparatus and in the extracellular space to produce a high diversity of HS chains^{45,46}. We anticipate that the structural diversity of heparan sulfates, together with the diversity of the proteoglycan core (perlecan, agrin, collagen XVIII) reflects the binding specificity for heparin-binding growth factors throughout the SVZ. The pattern of heparan sulfates and of their sulfation may provide specific instruction for capturing a given ligand that will mediate the specificity of ligand/receptor interactions and ultimately the biological activity promoted by the ligand. This hypothesis has been already successfully examined for axon guidance⁴⁷.

Supporting the strong implication of heparan sulfates in other stem cell niches, it has been recently demonstrated in vitro that heparan sulfates act as promoters of mesenchymal stem cell proliferation and differentiation⁴⁸. It is now important to determine whether the macrophage/microglia associated with fractones and with the SVZa perivasculature^{1,2} produce HSPG and control the dynamic information encoded within fractones to control cell division. Macrophage/microglia can produce HSPG^{42,49} and are involved in the process of adult neurogenesis⁵⁰.

Conclusions

Fractones and specialized vascular basement membranes were found to be essential for the regulation of cell division by BMP-7 and FGF-2 in the adult neural stem cell niche. This is the first characterization of fractone function. Moreover, our experiments suggest that heparan sulfates, and particularly those that are N-sulfated, may be crucial chemical effectors of fractones and SVZ basement membranes, providing specific ability for growth factor capture and activation. This makes the SVZ and its ECM components (fractones and basement membranes) unique and particularly suitable for recruiting and dispatching growth factors/cytokines originating from the ventricular cavities. Therefore, we propose that fractones along the brain ventricular system, i.e. lateral, third, and fourth ventricles, aqueducts and spinal canal, act as captors of signaling ligands, selecting and potentiating the ligand functions at a precise and controlled location to ultimately organize multiple biological processes, including adult neurogenesis in the SVZa and other neural regulatory functions in the rest of the ventricular system.

Acknowledgements

We thank Aurelien Kerever for technical assistance, and Tina Carvahlo, Marilyn Dunlap, Tom Humphreys and Brandon Pearson for reviewing previous drafts of this manuscript. We acknowledge the Histology and Imaging Core of the Cell and Molecular Biology Department of the John A Burns School of Medicine, University of Hawaii, supported by the NIH G12-RR003061 and P20-RR016453. This work was supported by National Institutes of Health (NIH) grants R21 NS057675 and NCR5 G12 RR/AI03061, including RCMI Clinical and Translational Science Bridging Funds. We particularly thank Eri-Arikawa-Hirasawa, Juntendo School of Medicine, Tokyo, our collaborator, for scientific and technical support, as well as the Japanese Society for the Promotion of Science, for travel awards.

FIGURES

Figure 1. Structure, ultrastructure and distribution of fractones in the adult mammalian brain. **(a)** Schematic representation of a fractone. The fractal structure allows an individual fractone (green) to contact the processes of numerous neighboring cells (red). **(b)** Ultrastructure of an

individual fractone (arrow) visualized by transmission electron microscopy in the subventricular zone (SVZ) of the adult rat. Note the multi-branched (fractal) structure. (c) A fractone contacts multiple glial and neural stem cell processes (arrows) in the SVZ covering the corpus callosum (CC). (d) Fractones appear as punctae (green) in light microscopy after immunolabeling for N-sulfated heparan sulfates (NS-HS). Cell nuclei are counterstained with DAPI (blue). Some vascular basement membranes in the SVZa are labeled for NS-HS (green) and laminin alpha-1 (red). (e) Schematic representation of the adult neurogenic zone in the SVZ of the lateral ventricle (LV). Fractones (green) are associated with proliferating neuroblasts/neural stem cells (red) in the SVZa. Note that the fractones directly contact ependymocytes (Ep), the first cell layer of the ventricle wall. Cp: choroid plexus; Ca: caudate nucleus. The inset indicates the location of images (c) and (d), and diagram (e). (f) Confocal imaging of the most active germinal niche of the adult brain. Adult mouse fractones (visualized by laminin-immunolabeling, green punctae, arrow) are associated with dividing cells (BrdU labeling, red) in the SVZ covering the Ca (the plane of section is tangential to the Ca surface). The inset shows the location of this image in a sagittal diagrammatic view of the brain. Scale bars. b and d: 1 μm ; E: 25 μm , h: 100 μm .

Figure 2. Fractones and SVZa basement membranes capture BMP-7. (a) 22 hours after ICV injection, biotinylated-BMP-7 was detected by streptavidin-Texas as multiple punctae (arrow) in the SVZ of the lateral ventricle (LV) and in the choroid plexus (CP). CPu: caudate putamen, CC: corpus callosum; FH: fimbria hippocampus. (b) Identification of the BMP-7 punctate binding sites as fractones (arrow) by 10E4 (NS-HS) immunolabeling (green). Note the strict correlation between the sites of binding for BMP-7 (a) and the immunoreactivity for 10E4 (b). (c) Magnification of the zone indicated by an arrow in image A, showing that not only fractones (arrowheads), but also blood vessels have captured BMP-7 (arrowheads showing truncated blood vessels). (d) Same section showing that these blood vessels are immunoreactive for NS-HS. (e) Location of images (a-d) in a sagittal representation of the brain. (f) After deglycanation by heparitinase-1, fractones cannot capture BMP-7 (absence of BMP-7 detection in the red channel). Absence of 10E4 immunolabeling (in the green channel) indicates that heparan sulfates have been cut. (g) Same field showing that deglycanation was not detrimental to the visualization of fractones by laminin immunoreactivity (Alexa-Fluor 647, displayed in clear-blue). (h) 22

hours after injection, biotinylated BMP-7 has also been captured by fractones of the fourth ventricle (arrow) and by meninges extending up to the fourth ventricle (arrowhead). Green: 10E4 immunolabel. **(i)**. Same image displaying BMP-7 binding (red) and cell nucleus counterstaining (blue). Scale bars. a and c: 1 μm ; b, f and g: 25 μm ; d, e, i: 100 μm .

Figure 3. BMP-7 must bind fractones and adjacent basement membranes to inhibit cell division in the SVZa neurogenic niche. **(a)** Cell division in the SVZa (coronal section) after two successive injections of artificial cerebrospinal fluid (CSF). Dividing cells were visualized by bromodeoxyuridine (BrdU) immunolabeling (green). Fractones and SVZa basement membranes were visualized by 10E4 immunolabeling (red). Magnified zones (insets) show that cells divide near fractones or vascular basement membranes (arrow). The location of images is indicated in **(d)** (between red arrows). **(b)** Cell division in the SVZa after two successive injections of BMP-7. BMP-7 has drastically decreased the number of dividing cells. The inset shows rare BrdU+ cells (green). **(c)** Cell division in the SVZa after two successive injections of heparitinase-1+ BMP-7. Heparitinase-1 prevented the inhibition of BMP-7 and restored cell proliferation in the SVZa (arrow in inset). **(d)** Top. Location of images. Bottom. Diagram reporting BrdU+ average cell counts per 25 μm -thick section in the different experimental conditions. Scale bars: 100 μm .

Figure 4. Fractones and SVZ basement membranes capture FGF-2. **(a)** Binding of biotinylated FGF-2 (red) revealed by streptavidin Texas red in a sagittal section 22 hours after ICV injection. FGF-2 was concentrated in the SVZ (arrow) and choroid plexus (arrowhead). **(b)** Same section showing immunolabeling for fractones and choroid plexus (10E4, green). The coincidence between FGF-2 binding and 10E4 immunolabeling indicates that FGF-2 has been concentrated in fractones (arrow) and the choroid plexus (arrowhead). The inset shows the location of the image. Ca: caudate nucleus; CC: corpus callosum; LV: lateral ventricle. **(c)** 2.8x magnification of the area indicated by an arrow in **(a)**, showing both FGF-2 binding and 10E4 immunolabeling. Nearly all fractones have bound FGF-2 (appear yellow by double labeling) (arrow). Note that vascular basement membranes immunoreactive for 10E4 have bound FGF-2 (arrowhead). Scale bars. a: 100 μm ; c: 50 μm .

Figure 5. FGF-2 capture by fractones and basement membranes is independent of the injection site. **(a-c)** Binding of FGF-2 visualized by streptavidin Texas red in the SVZ of the third ventricle, 22 hours after ICV injection. FGF-2 binding (red) and immunolabeling for laminin (blue), 10E4 (green) and are all displayed in the image a. Image (b) shows 10E4 only and image (c) shows FGF-2 binding only. Due to the construction of the third ventricle, fractones appear as two parallel lines (arrows). Numerous fractones (arrow in b) have captured and concentrated biotinylated FGF-2 (arrow in c). Specific blood vessels of the SVZ have captured FGF-2 (double arrow). Most blood vessels did not (arrowheads). The inset indicates the location of images. **(d-f)** 22 hours after injection of biotinylated FGF-2 in the dorsal cortex, 10E4 immunolabeling (green, in d) and binding of biotinylated FGF-2 (red, in f) are found in fractones of the lateral ventricle SVZ. FGF-2 binding and 10E4 are displayed together in (e). Fractones of the lateral ventricle SVZ wall have concentrated FGF-2 (arrows in e and f). Note that the choroid plexus also concentrated FGF-2. The inset in d indicates the location of images. Scale bars: 100 μ m.

Figure 6. The binding of FGF-2 to fractone-heparan sulfates and vascular basement membranes is heparin-binding dependant. **(a)** Absence of biotinylated-FGF-2 binding (streptavidin Texas red) 22 hours after ICV injection of biotinylated-FGF-2 and heparitinase-1. No labeling is visible in the SVZ (arrow). Note the faint binding in the choroid plexus stroma (arrowhead) **(b)** Same section showing immunolabeling for N-sulfated HS (antibody 10E4). No 10E4 labeling is visible in the SVZ or other zones of the brain parenchyma, indicating that heparitinase-1 deglycanation was effective. Note that deglycanation was not effective beyond the brain barrier in the choroid plexus stroma (arrowhead). **(c)** Schematic representation of the brain (sagittal plane, 1.3 mm to the midline). The arrow indicates the location of the images a, b. **(d)** Recovery of HSPG chains (10E4 immunoreactivity, green) 48 hours after ICV injection of heparitinase-1. The red punctae indicate the nuclei of proliferating cells (immunolabeling for BrdU) next to fractones (green punctae, arrow) in the SVZ neurogenic zone. Scale bars: 100 μ m.

Figure 7. The binding of FGF-2 to fractones is required for the stimulation of cell division in the SVZ. **(a, c, d, f)** Coronal sections showing the index of cell proliferation (BrdU+, red) in the anterior SVZ after ICV injections of FGF-2 (a), CSF (c), heparitinase-1 plus FGF-2 (f) or heparitinase-1 only (d). Cell division was strongly stimulated by FGF-2 (arrow and arrowhead in

a; compare a and c). The location of the lateral ventricle, narrow in this location (Bregma + 1mm) is indicated by a double arrow. **(b)** Inset showing a x2.5 magnification of the zone indicated by an arrow in (a). The right inset indicates the location of images a-f (red arrow). Both left and right ventricles are displayed in (a). Cell division was not substantially induced by FGF-2 when the binding of FGF was inhibited by heparitinase-1 (compare a and f), suggesting that FGF-2 binding to fractones was required to stimulate cell proliferation in the SVZ. **(e)** Diagram reporting the average number of proliferating (BrdU+) cells per section per lateral ventricle wall (left or right) upon the different experimental conditions. The numbers represent the averages of all sections counted (not the number of cells included in the displayed images). Scale bars: 100 μm .

Figure 8. Interpretation of the results: Fractones and its heparan sulfates as captors, selectors and dispatchers of growth factors in the neurogenic zone. **(a)** FGF-2 and BMP-7, which circulate in the cerebrospinal fluid of ventricles, enter through interstitial clefts in between ependymocytes. **(b)** FGF-2 and BMP-7 are captured by the heparan sulfates of fractones. **(c)** Fractone-heparan sulfates target FGF-2 and BMP-7 towards selected cells in the SVZ and facilitate growth factor binding to their cognate receptors at the surface of target cells. **(d)** FGF-2 and BMP-2 have docked to their respective cell-surface receptors on selected cells. **(e)** Promoted by heparan sulfates, FGF-2 engages mitosis of the targeted cell, whereas BMP-7 blocks the division of the other cell. **(f)** Mitosis of the cell targeted by FGFG-2 occurred.

References

1. Mercier, F., Kitasako, J.T. & Hatton, G.I. Anatomy of the brain neurogenic zones revisited: fractones and the fibroblast/macrophage network. *J. Comp. Neurol.* **451**, 170-188 (2002).
2. Mercier, F., Kitasako, J.T. & Hatton, G.I. Fractones and other basal laminae in the hypothalamus. *J. Comp. Neurol.* **455**, 324-340 (2003).
3. Timpl, R. Structure and biological activity of basement membrane proteins. *Eur. J. Biochem.* **180**, 487-502 (1989).

4. Yurchenko, P.D. & Schittny, J.C. Molecular architecture of basement membranes. *FASEB J.* **4**, 1577-1590 (1990).
5. Linsenmayer, T.F. Collagen. In *Cell biology of extracellular matrix*, ed. E. D. Hay, Plenum press, pp. 7-44, 1991.
6. Reitsma, S., Slaaf, D.W., Vink, H., van Zanvoort, M. A. M. J. & oude Egbrink, M.G.A. The endothelial glycocalyx: composition, functions and visualization. *Pflugers Arch.* **454**, 345-359 (2007).
7. Mandelbrot, B.B. in *The fractal geometry of nature*, ed. B. B. Mandelbrot, San Francisco, V. H. Freeman pp. 468, (1977).
8. Kerever, A. et al. Novel extracellular matrix structures in the neural stem cell niche capture the neurogenic factor FGF-2 from the extracellular milieu. *Stem Cells.* **25**, 2146-2157 (2007).
9. Timpl, R. et al. Laminin : a glycoprotein form basement membranes. *J. Biol. Chem.* **254**, 9933-9937 (1979).
10. Timpl, R., Wiedemann, H., van Delden, V., Furthmayr, H. & Kuhn, K. (1981). A network model for the organization of type-4 collagen molecules in basement membranes. *Eur. J. Biochem.* **120**, 203-211 (1981).
11. Kato, M., Koike, Y., Suzuki, S. & Kimata, K. Basement membrane proteoglycan in various tissues: characterization using monoclonal antibodies to the Engelbreth-Holm-Swarm mouse umor low density heparan sulfate proteoglycan. *J. Cell. Biol.* **106**, 2203-2210 (1988).
12. Seaberg, R.M. & van der Kooy, D. Adult rodent neurogenic regions: The ventricular subependyma contains neural stem cells, but the dentate gyrus contains restricted progenitors. *J. Neurosci.* **22**, 1784-1793 (2002).

13. Weiss, S. et al. Multipotent CNS stem cells are present in the adult mammalian spinal cord and ventricular neuroaxis. *J. Neurosci.* **16**, 7599-7609 (1996).
14. Altman, J. Autoradiographic and histological studies of postnatal neurogenesis. IV. Cell proliferation and migration in the anterior forebrain with special references to persisting neurogenesis in the olfactory bulb. *J. Comp. Neurol.* **137**, 433-458 (1969).
15. Das, G.D. & Altman, J. Postnatal neurogenesis in the caudate nucleus and nucleus accumbens septi in the rat. *Brain Res.* **21**, 122-127. (1970).
16. Lois, C. & Alvarez-Buylla, A. Proliferating subventricular zone cells in the adult mammalian forebrain can differentiate into neurons and glia. *Proc. Nat. Acad. Sci.* **90**, 2074-2077 (1993).
17. Doetsch, F., Garcia-Verdugo, J.M. & Alvarez-Buylla, A. Cellular composition and three dimensional organization of the sub-ventricular zone in the adult mammalian brain. *J Neurosci.* **17**, 5046-5061. (1997).
18. Lois, C. & Alvarez-Buylla, A. Long distance neuronal migration in the adult mammalian brain. *Science* **265**, 1145-1148 (1994).
19. Gordon, M.Y., Riley, G.P., Watt, S.M. & Greaves, M.F. Compartmentalization of an hemopoietic growth factor (GM-CSF) by glycosaminoglycans in the bone marrow microenvironment. *Nature* **326**, 403-405 (1987).
20. Roberts, R. et al. (1988). Heparan-sulfate-bound growth factors : a mechanism for stromal cell mediated hematopoiesis. *Nature* **332**, 376-378 (1988).
21. Yayon, A., Klagsbrun, M., Esko, J.D., Leder, P. & Ornitz, D.P. (1991). Cell surface, heparin-like molecules are required for binding of basic fibroblast growth factor to its high affinity receptor. *Cell*

64, 841-848 (1991).

22. Aviezer, D. et al. Perlecan, basal lamina proteoglycan, promotes basic fibroblast growth factor-receptor binding, mitogenesis and angiogenesis. *Cell* **79**, 1005-1013 (1994).

23. Reiland, J. & Rapraeger, A.C. Heparan sulfate proteoglycan and FGF receptor target basic FGF to different intracellular destinations. *J. Cell Sci.* **105**, 1085-1093 (1993).

24. Miyazaki, T. et al. Oversulfated chondroitin sulfate-E binds to BMP-4 and enhances osteoblast differentiation. *J. Cell. Physiol.* **217**, 769-77 (2008).

25. Mercier, F. and Hatton, G.I. Immunocytochemical basis for a meningeo-glial network. *J. Comp. Neurol.* **420**, 445-465 (2000).

26. Mercier, F. & Hatton, G.I. Meninges and perivasculature as mediators of CNS plasticity. In: Non neuronal cells in the nervous system: Function and dysfunction. Bittar, E.E., Herz, I., eds. Amsterdam, Elsevier Bioscience. *Adv. Mol. Cell Biol.* **31**, 215-253 (2004).

27. Shou, J., Rim, P.C. & Calof, A.L. BMPs inhibit neurogenesis by a mechanism involving degradation of a transcription factor. *Nat. Neurosci.* **4**, 301-303 (1999).

28. Palmer, T.D., Ray, J. & Gage, F.H. FGF-2 responsive neuronal progenitors reside in proliferative and quiescent regions of the adult rodent brain. *Mol. Cell Neurosci.* **6**, 474-486 (1995).

29. Johansson, C.E. The choroid-plexus-CSF nexus: gateway to the brain. In Neuroscience in Medicine. Conn, P.M. eds, Humana Press, pp. 165-195 (2003).

30. Hayamizu, T.F., Chan, P.T & Johanson, C.E. FGF-2 immunoreactivity in adult rat ependyma and choroid plexus: responses to global forebrain ischemia and intraventricular FGF-2. *Neurol. Res.* **23**, 353-358 (2001).

31. Stopa, E.G. et al. Choroid plexus growth factors: what are the implications for CSF dynamics in Alzheimer's disease? *Exp. Neurol.* **167**, 40-47 (2001).
32. Mertens, G., Cassiman, J.J., Van den Berghe, H., Vermylen, J. & David, G. Cell surface heparan sulfate proteoglycans from human vascular endothelial cells. Core protein characterization and antithrombin III binding properties. *J. Biol. Chem.* **267**, 20435-20443 (1992).
33. Brickman, Y.G., Ford, M.D., Small, D.H., Bartlett, P.F. & Nurcombe, V. Heparan sulfates mediate the binding of basic fibroblast growth factor to a specific receptor on neural precursor cells. *J. Biol. Chem.* **270**, 24941-24948 (1995).
34. Vlodavsky, I. et al. Endothelial cell-derived basic fibroblast growth factor: synthesis and deposition into subendothelial extracellular matrix. *Proc. Nat. Acad. Sci.* **84**, 2292-2296 (1987).
35. Tsen, G., Halfter, W., Kroger, S. & Cole, G.J. Agrin is a heparan sulfate proteoglycan. *J. Biol. Chem.* **270**, 3392-3399 (1995).
36. Muragaki, Y. et al. Mouse Col18a1 is expressed in a tissue-specific manner as three alternative variants and is localised in basement membrane zones. *Proc. Nat. Acad. Sci.* **92**, 8763-8767 (1995).
37. Guimond, S. Maccarana, M. Olwin, B.B. Lindhal, U. & Rapraeger, A.C. Activating and inhibitory heparin sequences for FGF-2 (basic FGF). Distinct requirements for FGF-1, FGF-2, and FGF-4. *J. Biol. Chem.* **268**, 23906-23914 (1993).
38. Nurcombe, V. Ford, M.D, Wildshut, J.A. & Barlett, P.F. Developmental regulation of neural response to FGF-1 and FGF-2 by heparan sulfate proteoglycan. *Science* **260**, 103-106 (1993).
39. Thorne, B.A. & Plowman, G.D. (1994). The heparin-binding domain of amphiregulin necessitates the precursor pro-region for growth factor secretion. *Mol. Cell. Biol.* **14**, 1635-1646 (1994).

40. Dierker, T., Dreier, R., Petersen, A., Bordych, C. & Grobe, K. Heparan sulfate-modulated, metalloprotease-mediated sonic hedgehog release from producing cells. *J. Biol. Chem.* **284**, 8013-8022. (2009).
41. Hienola, A., Pekkanen M, Raulo, E., Ventolla, P. & Rauvala, H. HB-GAM inhibits proliferation and enhances differentiation of neural stem cells. *Mol. Cell Neurosci.* **26**, 75-88 (2004).
42. Jin, K., Zhu, Y Sun, Y., Mao, X.O., Xie, L. & Greenberg D.A. Vascular endothelial growth factor (VEGF) stimulates neurogenesis in vitro and in vivo. *Proc. Nat. Acad. Sci.* **99**, 11946-11950 (2002).
43. Lai, K., Kaspar, B.K., Gage, F.H. & Schaffer, D.V. Sonic hedgehog regulates adult neural progenitor proliferation in vitro and in vivo. *Nat. Neurosci.* **6**, 21-27 (2003).
44. Abramsson, A. et al. Defective N-sulfation of heparan sulfate proteoglycans limits PDGF-BB binding and pericyte recruitment in vascular development. *Genes Dev.* **21**, 316-331 (2007).
45. Esko, J.D. & Lindahl, U. (2001). Molecular diversity of heparan sulfate. *J. Clin. Invest.* **108**, 169-73.
46. Presto, J. et al. Heparan sulfate biosynthesis enzymes EXT1 and EXT2 affect NDST1 expression and heparan sulfate sulfation. *Proc. Nat. Acad. Sci.* **105**, 4751-4756 (2008).
47. Bulow, H.E. et al. Extracellular sugar modifications provide instructive and cell-specific information for axon guidance choices. *Current Biol.* **18**, 1976-1985 (2008).
48. Dombrowski, C. et al. Heparan sulfate mediates the proliferation and differentiation of rat mesenchymal stem cells. *Stem Cells Dev.* **18**, 661-670 (2009).

49. Miller, J.D. et al. Localization of perlecan (or a perlecan-related macromolecule to isolated microglia in vitro and to microglia/macrophages following infusion of beta-amyloid protein into rodent hippocampus. *Glia* **21**, 228-243 (1997).

50. Butovsky, O. et al. Microglia activated by IL-4 & IFN- γ differentially induce neurogenesis and oligodendrogenesis from adult stem/progenitor cells. *Mol. Cell. Neurosci.* **31**, 149-160. (2006).

Materials and Methods

Animals

8-10 week old male and female Balb/c mice (n=60) were injected intraperitoneally with bromodeoxyuridine (BrdU) (50mg/kg of body weight) (Sigma; St. Louis, MO) and stereotaxically into the lateral ventricle (ICV injection, 0.6 mm lateral to the midline, 2 mm depth from the dorsal pia) or in the dorsal cortex (2 mm lateral to the midline, 1.5 mm depth from the dorsal pia) with heparitinase-1 (32mU/injection, from Flavobacterium heparinum, Seikagaku, Japan), FGF-2 (0.5 μ g/animal) (Chemicon/InVitrogen, Carlsbad, CA), BMP-7 (0.5 μ g per animal) (10-783-79729, GenWay Biotech, Inc, San Diego, CA). The animal experimental protocol followed NIH guidelines and was approved by the Institutional Animal Care and Use Committee at the University of Hawaii.

In vivo binding of FGF-2 and BMP-7

FGF-2 and BMP-7 were biotinylated as described in the EZ-link Micro-sulfo- NHS Biotinylation kit, 21425, Pierce, Rockford, IL). 0.5 μ g of each biotinylated growth factor was diluted in artificial cerebrospinal fluid (Harvard Apparatus, Holliston, MA) and injected by stereotaxy (intracerebroventricularly or in the dorsal cortex), following or not heparitinase-1 injection. The binding sites of growth factors were revealed on brain frozen sections with streptavidin-Texas red. When ICV injections of biotin only or artificial CSF only were carried out, no streptavidin Texas red signal was detected in the brain. Native recombinant and biotinylated-FGF-2 and -BMP-7 were equally active on cell proliferation in the SVZ of the lateral ventricle. As a negative control, we injected non-conjugated biotin into animals. Controls did not show any detectable label after streptavidin Texas red labeling on frozen sections (data not shown).

Microscopy

The results were recorded with a Zeiss Pascal confocal laser scanning microscope or a digital DFC350FX Leica camera mounted on a Leica DMIL epifluorescence microscope. In both cases, Plan Apo dry objectives were used. Images were processed with Adobe Photoshop CS3 (Adobe Systems, Mountain view, CA). Numerous images displayed (such as Figs. 4A and B, 6E) originate from X-Y montages of single images captured with a high magnification objective. This allowed us to obtain large fields of view, with a high resolution. Adjustments for brightness and contrast were not done or were minimal. Transmission electron microscopy was performed as previously published^{1,25}.

Effect of injecting FGF-2, BMP-7, combined or not with heparitinase-1 on cell proliferation in the SVZ

The ICV injections of FGF-2, BMP-7 and/or heparitinase-1 diluted in artificial CSF were performed as two subsequent 15 minute-injections in series of four adult mice at day 1, repeated at day 3, and the mice were terminated at day 5. The different experimental conditions were as follows: CSF + CSF (two subsequent injections of CSF termed CSF condition), CSF + of 0.5 µg of growth factor (FGF-2 or BMP-7 condition), heparitinase-1 + growth factor (Hep + FGF-2 or BMP-7 condition), or heparitinase-1 + CSF (Hep alone condition). BrdU was injected once six hours prior to the animal termination, to detect the majority of cells in S phase mitosis, and BrdU immunolabeling performed in series of sagittal or coronal whole brain sections. BrdU+ cells were directly counted under the fluorescence microscope using a x20 PlanApo objective in serial coronal sections including the SVZ of the lateral ventricle or in serial sagittal sections including the SVZ.

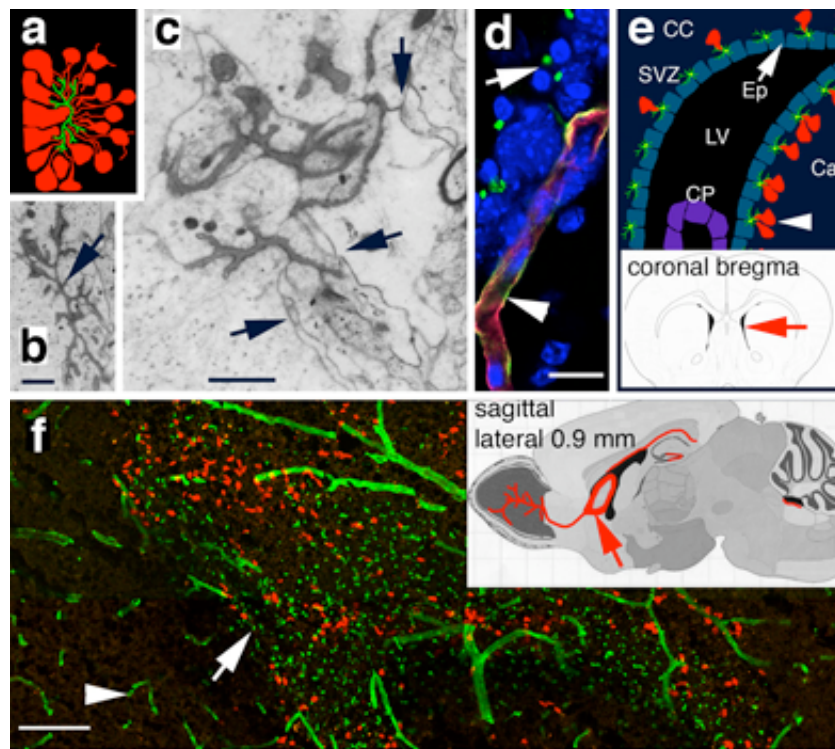
Immunocytochemistry

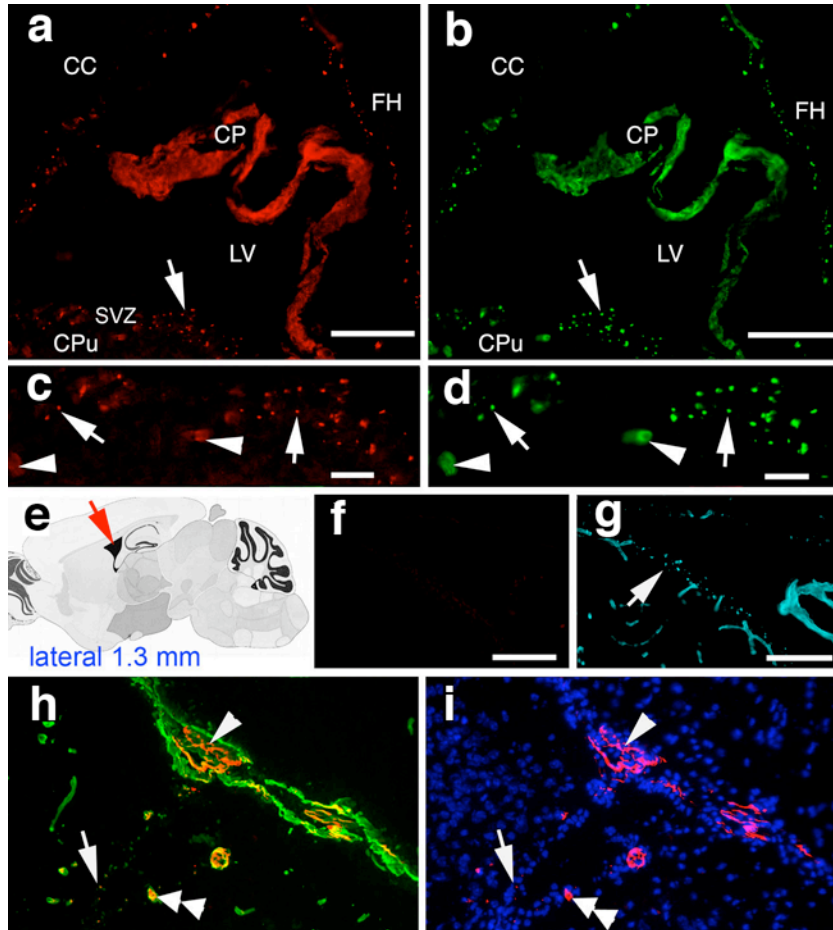
The immunocytochemistry procedures were performed as described²⁵ on serial frozen sections fixed with acetone at -20C. Subsequent immunolabeling with an additional 4% PFA fixation prior to 2NHCL treatment was used for BrdU immunocytochemistry. Fractones, blood vessels and choroid plexus were labeled with the anti-laminin antibody (L9393, Sigma, St. Louis, MO) or the anti-N-sulfate glycosamine antibody (10E4, Seikagaku, Japan), then visualized with

donkey anti-rabbit conjugated to fluorescein isothiocyanate (FITC) (N1034VS, Amersham, Piscataway, NJ) and goat anti-mouse IgM conjugated to Alexa Fluor 488 (A21042, InVitrogen, Carlsbad, CA) or donkey anti-mouse IgM conjugated to Cy-3 (Jackson Laboratories, Bar Harbor, ME), respectively. Pre-mitotic cells (S-phase) were labeled with anti-BrdU antibodies (OBT0030, Oxford Biotechnology, UK) as described in ⁹, and visualized with goat anti-rat Alexa- Fluor 546 or goat anti-rat conjugated to AlexaFluor488 (Molecular Probes/InVitrogen, Carlsbad, CA).

Cell counts and statistical Methods

BrdU+ cells were counted throughout series of whole-brain 25- μ m thick coronal and 14 μ m-thick sagittal sections. The serial brain frozen sections were generated with a Leica CM1900 cryostat and were all identified according to their bregma or lateral coordinates. Cell counts and means were calculated and reported per segment of 0.1 mm (supplementary tables 1 and 2). For coronal sections, BrdU+ cells counts are reported per lateral ventricle wall. No differences were observed between the ventricles located ipsi- and contralateral to the injection site. For sagittal sections, cells counts were performed on the SVZ only. Cell division in the rostral migratory stream was excluded by anatomical landmarks and by the absence of fractones, indicated by the lack of laminin-immunoreactive punctae. The cell proliferation numbers (BrdU+cell numbers) were averaged separately for each condition with the respective standard deviation of the means, and analyzed by a one-way ANOVA ($\alpha= 0.05$) followed by a Turkey's test and a two-sided Dunnett's test to compare each condition to the control (CSF conditions). Multiple comparison tests were made by the REQWQ's procedure. XLStat was used for all analyses. Differences between two groups were considered significant when $p<0.001$.





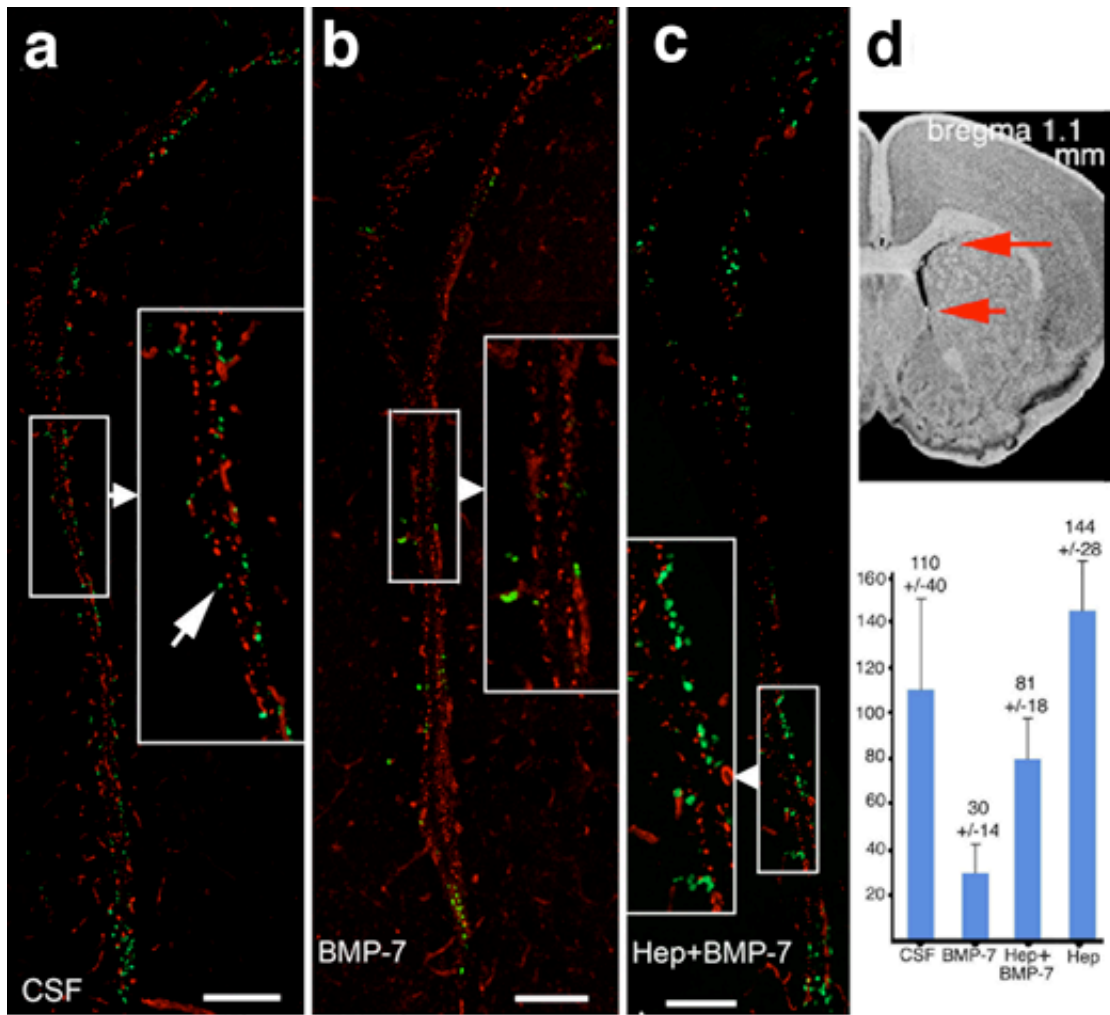
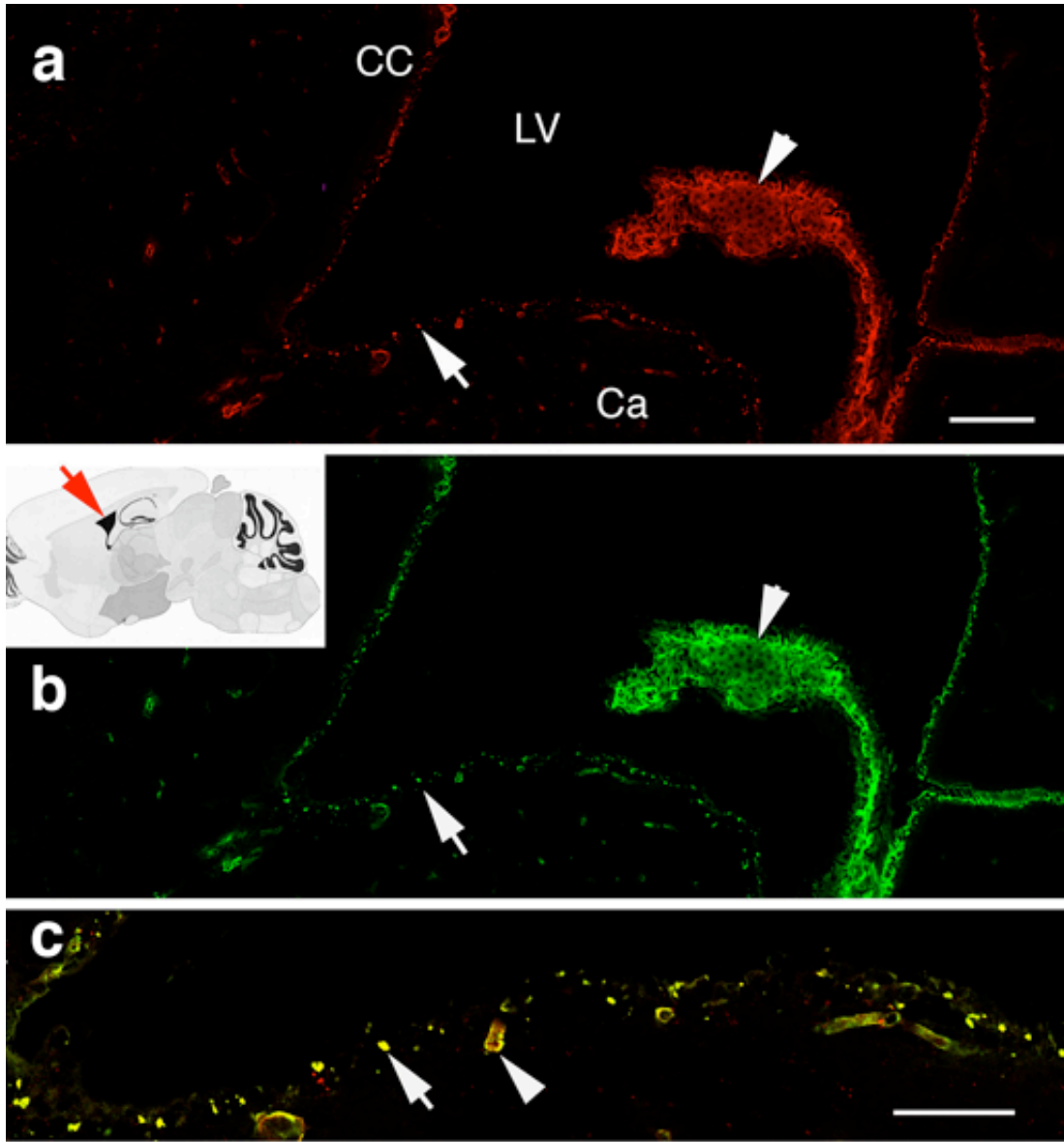
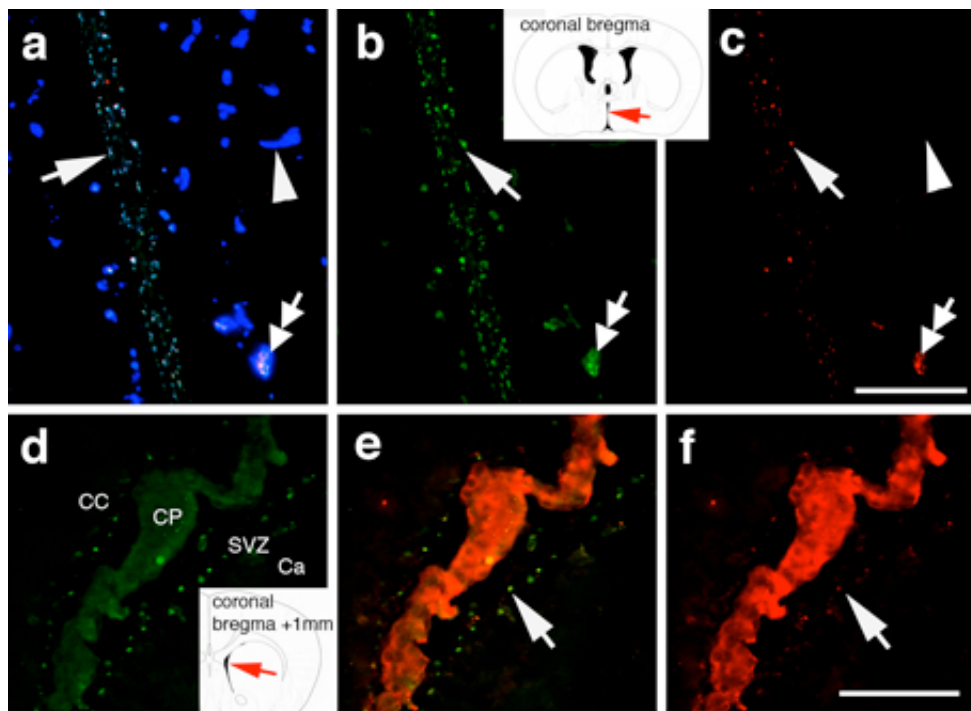


Figure 3, Mercier





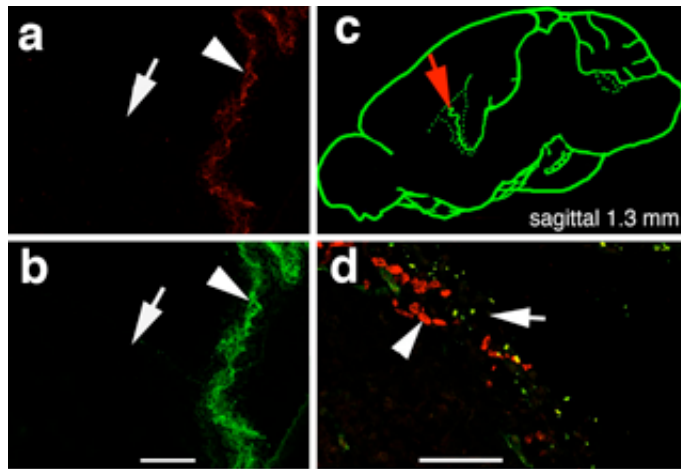


Figure 6, Mercier

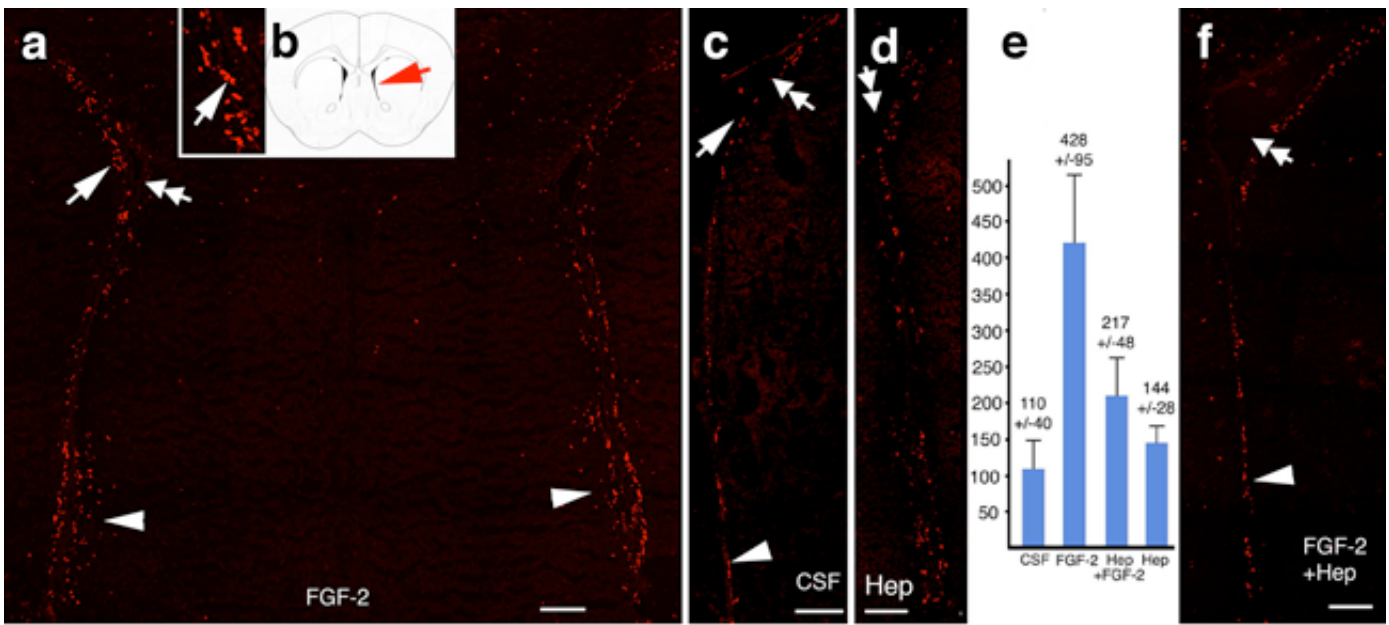


Figure 7, Mercier

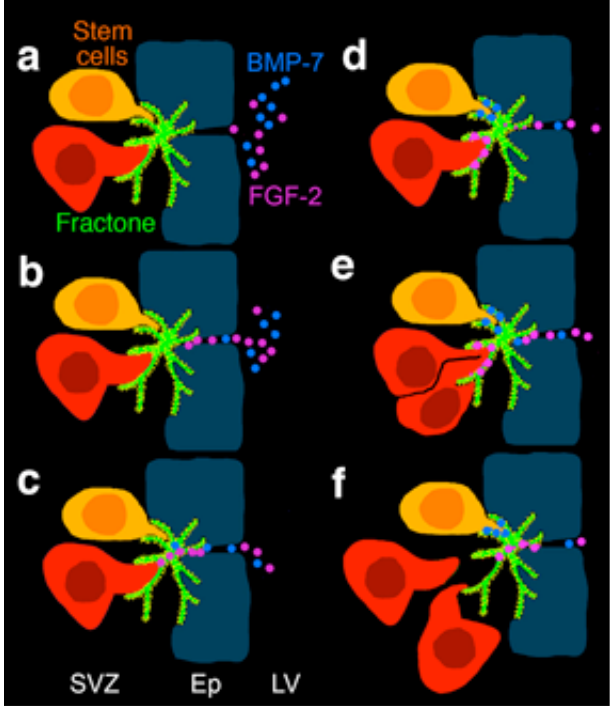


Figure 8, Mercier